First year Research Project

Understanding heterochromatin redistribution in mouse retina

by designing and implementing a novel reporter cell-line in retinal organoids

Simona Ivanova Ivanova

Student number: 8992509

Master's program: Science and Business Management

Utrecht University

Academic Year: 2022-2023

Examiner: Prof. Dr. Jop Kind (Hubrecht Institute)

Daily supervisors: Dr. Robin van der Weide and Dr. Moritz Bauer (Hubrecht Institute)

Second reviewer: Dr. Catherine Robin (Hubrecht Institute)

Abstract

In eukaryotic cells, DNA is packed in the form of chromatin distributed three-dimensionally. This allows for the control of gene expression based on the location of chromatin. Euchromatin is transcriptionally active and located at the nuclear interior, while heterochromatin is transcriptionally inactive and found at the nuclear periphery. This is known to be the conventional organization and is found across vertebrates. However, mature nocturnal rod photoreceptors in the retina have the opposite nuclear organization. Hence, euchromatin is located at the nuclear periphery and heterochromatin at the nuclear interior. The purpose of this project is to optimize and develop tools to study the rod-specific nuclear organization.

The Kind-lab developed the scDam&T approach, which allows for the simultaneous measurement of genomic positioning and transcription in single cells. Combining this method with an mESC-based in vitro organoid system would allow us to study and perturb the inversion. However, preliminary data showed that the Dam-LaminB1 F1ES line could not differentiate into retinal organoids. First, I optimized the mouse retinal organoid protocol and tested multiple cell lines. Next, we generated an inducible IB10-based Dam-LaminB1 cell line. From this we were able to grow organoids which showed all the hallmarks of retinal organoids.

Table of Contents

Introduction

The retina

An important layer of the eye is the retina. Located at the posterior section, between the vascular choroid and the fibrous sclera (Nguyen et al., 2022). The retina has a striking layered organization. Specifically, the photoreceptor layer is composed of polarized sensory neurons known as rods and cones. The function of this layer is to transform photons into action potential signals (Nguyen et al., 2022). Consequently, neurons of the layers between the outer plexiform layer (OPL) and retinal ganglion cells (RGC) transmit and transform the signal. From there the signal moves from the nerve fiber layer (RNF) to the brain. Apart from photoreceptor cells, there are a variety of cell types comprising the retinal tissue, including bipolar cells, ganglion cells, horizontal cells and amacrine cells (Bellapianta et al., 2022).

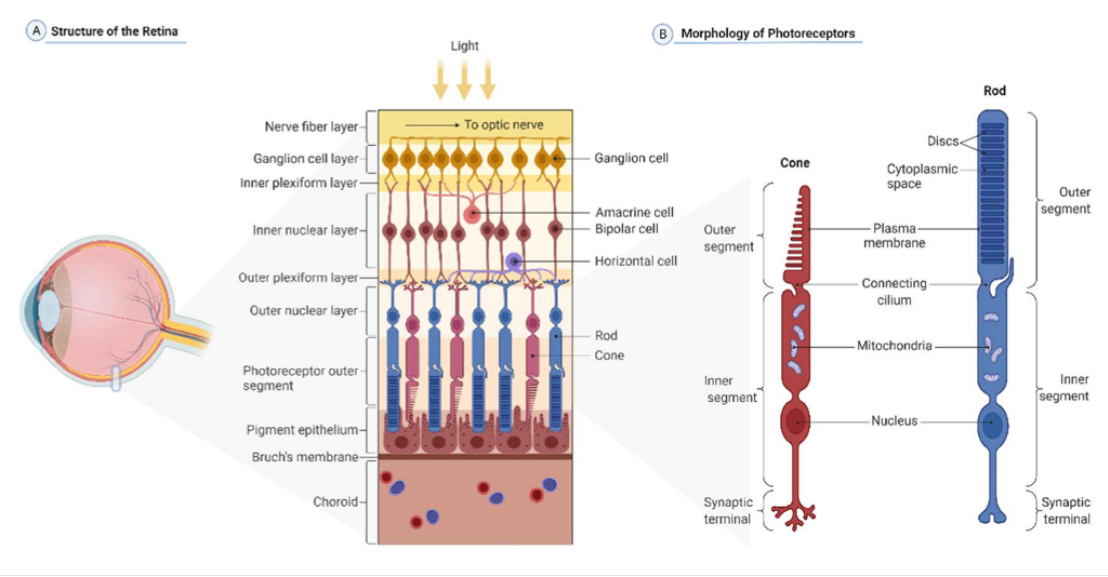

Figure 1. **A**. Layer and cellular organization of the retina. **B**. Structure of cones and rods photoreceptors. Taken from (Bellapianta et al., 2022).

A look into the nuclear organization

The DNA of eukaryotic cells is packed as chromatin and arranged in subnuclear compartments (Misteli, 2007). This compartmentalization enables the effective control of gene expression by separating transcriptionally active chromatin, known as euchromatin and the transcriptionally silent heterochromatin in three-dimensional space (Huisinga et al., 2006) (Zheng & Xie, 2019). Typically, the less condensed euchromatin is located in the nuclear interior, whereas the dense heterochromatin is located at the nuclear lamina (NL) and around nucleoli (Huisinga et al., 2006) (Misteli, 2020). The nuclear lamina is a meshwork containing A- and B-type lamins at the inner face of the nuclear membrane (Kind & van Steensel, 2010; Shevelyov & Ulianov, 2019) (Hoskins et al., 2021). The nuclear lamina supports the nucleus structurally and participates in several nuclear processes, including chromatin arrangement and gene control (Briand & Collas, 2020). Lbr and Lmna are two crucial genes that bind heterochromatin to the nuclear lamina (Solovei et al., 2013) . LBR, a crucial protein for the inner nuclear membrane, is encoded by this gene (Solovei et al., 2009). Lamins A and C (LamA/C) are produced by Lmna and serve as a scaffold for proteins that interact with chromatin(Solovei et al., 2013).

Moreover, there are specific areas of the genome known as lamina-associated domains (LADs) linked to the NL (van Steensel & Belmont, 2017). LADs have a role in gene regulation, genome organization, and nuclear function (Lochs et al., 2019). This is why, is important to understand the properties and dynamics of LADs .

Molecular adaptation to nocturnalism

While this conventional organization is found across vertebrates, mature nocturnal rod photoreceptors harbor the complete opposite organization (Carter-Dawson & LaVail, 1979). Rod cells of nocturnal mammals have heterochromatin located at the center of the nucleus and the active transcription factors at the nuclear periphery, thereby increasing light sensitivity (Smith et al., 2021) (Ragoczy & Groudine, 2009). In mice, the inversion happens during the first postnatal month (Nguyen et al., 2022; Solovei et al., 2009).
This inversion brings us to an important question about the function of the conventional organization. Is heterochromatin-localisation at the periphery necessary? What is the role of repositioning to and from the lamina on transcription? What did the nocturnal animals lose in terms of gene regulation by having the nocturnal-permissive inverted organization?

Tracking inversion

In order to answer these questions, we need to measure the location and transcription of each genomic region per cell. The Kind-lab invented the scDam&T approach to do just that (Markodimitraki et al., 2020) (Orian et al., 2009; Rooijers et al., 2019) (Shevelyov & Nurminsky, 2012). It relies on a Dam methyltransferase fused to a nuclear envelope protein (Völkner et al., 2021)(like Lamin B1) located at the nuclear periphery (Greil et al., 2006). Previous work in the lab has shown that this works *in vivo*, but had limited success in the retina. Therefore, an analogous *in vitro* model like organoids could be a way to study the inversion like *in vivo*, but also would allow for more experimentation (Osakada et al., 2008) (Osakada et al., 2008). Organoids are an effective *in vitro* model because they are of their easy reproducibility and maintenance. Hence, using mouse retinal organoids is a solid testbed for our research questions.

However, preliminary data from the Kind group showed that F1ES cells could not differentiate into retinal organoids. Consequently, in this project, I aim to optimize the generation and culturing of mouse retinal organoids and introduce the Dam-Lamin B1 construct to study the inversion in vitro. This will allow us to track position and expression per gene in single cells, enabling the study of onset and maintenance of rod-specific chromatin inversion.

Materials & methods

Embryonic stem cell culture

The IB10 mouse embryonic stem cell (mESC) line, (a subclone of the E14 ES cell line), a kind gift from Luca Braccioli of the Elzo de Wit lab, was used in this study. Of note, this IB10 clone used to be cultured routinely in 2i/L media. Here, IB10 were cultured on gelatin-coated 6-well

plates in 2 ml/well Serum+LIF mESC medium. mESC medium contained G-MEM (Gibco, 21710-025) medium supplemented with 10% FBS (Sigma F7524), 1x GlutaMax^{TM}-I (Gibco, 35050-038), 1x Sodium Pyruvate (Thermo Fisher Scientific, 11360070), 1x Non-essential Amino Acids Solution (Thermo Fisher Scientific, 11140050), 10.000 U/ml Penicillin/Streptomycin (Gibco 15140-122), 0.1 mM β-mercaptoethanol (Sigma, M3148-100ML), 1,000 U/ml LIF (ESGRO® mLIF Medium Supplement). The medium was changed daily and dissociation was done with 500µl of TrypLE (Gibco, Stable Trypsin Replacement Enzyme, 12605-010) per 6-well. Cells were cultured in a humidified incubator at 37ºC in 5% CO_2, and were routinely tested for mycoplasma.

Retinal Organoid Differentiation

Day -4 to 0: mESC pre-culture

Mouse stem cell pre-culture encompassed four days. On D-4 mESC were thawed. The following days, cells were split daily at a seeding density of $6x10^5$ cells/well. On D-2 and D-1, 1µM PD032591 was added to the medium.

D0: Aggregation

The differentiation protocol started on D0, after four days of pre-culture. First, cells were washed with PBS and dissociated with TrypLE for 3 minutes at 37ºC. To remove differentiating cells, a step akin to feeder depletion was performed. Three 6-well plates were merged and 1 ml of cell suspension was transferred to a gelatin-coated 15 cm plate with 15 ml of mESC medium and incubated for 40 minutes at 37ºC. Then, the supernatant was collected and the plate washed once with mESC medium and collected in the same vial.
The collected supernatant mix was then centrifuged for 3 minutes at 0.2 rcf. The pellet was resuspended with 10 ml of PBS with 1% FBS. Cells were centrifuged and washed again in 5 ml retinal differentiation medium (RDM). RDM contains G-MEM supplemented with 1x Sodium Pyruvate, 1x Non-essential Amino Acids Solution, 1.5% Knockout Serum Replacement (Gibco, 10828010), 10.000 U/ml Penicillin/Streptomycin, and 0.1mM β-mercaptoethanol. Cells were then centrifuged and resuspended in 1 ml of RDM. To achieve a seeding density of 3,000 cells per 100 µl (per well), a total of $3x10^5$ cells were added to 10 ml RDM to give sufficient cell suspension for 1 full 96-well plate.100 µl/well were then seeded in a 96-well low adhesion plate (Nunclon Sphera-Treated, U-Shaped-Bottom Microplates, ThermoFisher Scientific, 174925) using a multi-channel pipette. Aggregates were cultured in a humidified incubator at 37ºC in 5% CO_2.

D1: 2% Matrigel or Geltrex addition

240 µl Matrigel® (Growth Factor Reduced (GFR) Basement Membrane Matrix, Phenol Red-free, LDEV-free, 10 mL, Corning®, 9035003) or alternatively 240 µl Geltrex (Gibco, A1413201) were added to 1.8 ml of cold RDM per plate. 20 µl Matrigel/Geltrex solution were added to each well using a multichannel pipette, pipetting up and down 3 times to mix.

D7 Transfer to bacterial dishes

Using a 10 ml pipette, organoids were transferred from the 96-well plate to an uncoated 10 cm petri dish in retinal maturation medium 1 (RMM1). RMM1 consists of DMEM/F12, supplemented with 1x GlutaMax (Gibco, 31331-028)1x N2 supplement (Gibco, 17502-048) and 10.000 U/ml penicillin/streptomycin (Gibco, 15140-122). Aggregates were cultured in a humidified incubator at 37ºC in 5% CO_2 and 20% O_2.

D10 Trisection

On D10, aggregates were trisected using two surgical tweezers (figure 2). Trisection has to be done under the microscope with a 5x or 10x magnification. One tweezer holds the whole organoid in between while the second tweezer makes the cut from the extreme side next to the holding tweezers until the opposite side. Trisected aggregates were then cultured in retinal maturation medium 2 (RMM2) containing DMEM/F12 with GlutaMax complemented with 1x N2 supplement, 10.000 U/ml penicillin/streptomycin and 10% FBS. From D10 to D14 RMM2 was supplemented with 0.3µM EC23 (Tocris, retinoic acid receptor, 17150172).

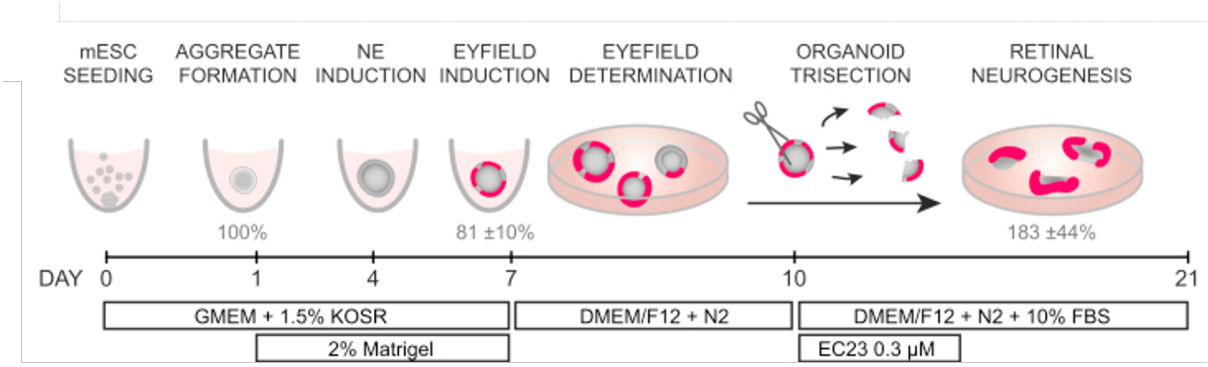

Figure 2. Schematic overview of the mROs culture. mESC aggregates are seeded on D0. Neuroepithelium induction occurs by D4. Organoids are transferred to bacterial dish on D7. Trisection on D10. Taken from (Völkner et al., 2016).

Continued culturing: D14- D40

From D14 onwards, RMM2 was changed periodically every 2-3 days.

Organoid harvesting and fixation

10 randomly selected single organoids were collected with a 10 ml pipette and washed with PBS. Organoids were fixed with 1 ml of 4% formaldehyde (diluted from 37% formaldehyde, Sigma-Aldrich, 605-001-00-5) for 30 minutes at room temperature. Subsequently, organoids were washed twice with PBS for 15 minutes each. Then, organoids were dehydrated using 25%, 50% and 70% ethanol for 15 minutes each. Finally, organoids were stored in 70% ethanol at 4ºC.

Hematoxylin and eosin stainings

Standard hematoxylin and eosin stainings were performed of the histological sections of fixed retinal organoids. Organoids were incubated for 5 minutes each in xylene and then 100% ethanol. This was followed by 1 minute incubation in ethanol of decreasing concentrations from 96%, 90%, 80%, 70%, 60%, 50% to 25%, respectively. Then 1 minute of incubation in distilled water. Next, the slides were incubated for 2 minutes with hematoxylin (Sigma-Aldrich, 1159380025) , followed by a 5-minute wash with tap water. Subsequently, one minute dehydrations with 50%, 60%, 70%, 80% and 90% ethanol solutions were done before the 2 minute incubation of eosin in 96% ethanol. Last, two incubations of two minutes each in 100% ethanol and xylene were performed before enclosing the slide with petrex and a coverslip.

DAPI stainings

Organoids were incubated for 5 minutes each in xylene and 100% ethanol. Then 1 minute incubation in ethanol 96%, 90%, 80%, 70%, 60%, 50%, 25% and distilled water respectively. Finally, slides were enclosed with coverslip and 2 drops of Antifade Mounting Medium with DAPI (VECTASHIELD HardSet^{TM}, H-1500). Stored in dark at 4ºC.

Quantitative RT-PCR

RNA was isolated (Macherey-Nagel, NucleoSpin RNA Kit, 740955.50) from 10 randomly selected single retinal organoids at specified time points (D15, D20, D25, D30, and D35). RNA was reverse transcribed into cDNA (Applied Biosystems, High-Capacity RNA-to-cDNA™ Kit, 4387406), using 10 µl of 2x RT Buffer Mix, 1 µl of 20x RT Enzyme Mix, and 9 µl of RNA. 20 µl cDNA was then diluted with 180 µl H_2O.

qRT-PCR was performed using the PowerUp™ SYBR™ Green Master Mix (Applied Biosystems, A25742) following the manufacturer instructions. 5 µl of PowerUp™ SYBR™ Green Master Mix, 0.2 µl of 10 µM Primer mix (forward and reverse primers), 2.8 µl of H_2O and 2µl of diluted cDNA were mixed. Analysis was performed in triplicate reactions on the same biological sample per time point.

Gene name	Forward primer (5'-3')	Reverse primer (5'-3')
Actb	CTAAGGCCAACCGTGAAAAG	ACCAGAGGCATACAGGGACA
Nrl	CCAAATCGCTACCTGTGGTT	GGGAACTCATCTCCAGCAAA
Crx	TTCCAGCGGAATCACTCTTT	GAAGGAGCCACTTTCATTGC
Neurod6	ATGCGACACTCAGCCTGAAA	CTGGGATTCGGGCATTACGA
Vsx2	CTCCGATTCCGAAGATGTTTCC	ATCTGGGTAGTGGGCTTCATT
Sox9	GTACCCGCATCTGCACAAC	TCCACGAAGGGTCTCTTCTC
Gapdh	ATGAATACGGCTACAGCAACAG G	CTCTTGCTCAGTGTCCTTGCTG
Pax6	CTGGAGAAAGAGTTTGAGAGG	TGATAGGAATGTGACTAGGAG
Arr3	ACTCCTGGCTGCCAACTGTCAG	GCTCCTTGTTCATTCCAGGTCG
Rho	TGCCACACTTGGAGGTGAAATC	ATGCGGGTGACTTCCTTCTCTG
Rcvrn	TACGACGTAGACGGCAATGG	TCCTCCTCTGTAAGTTTATCATCCT

Table 1. List of primers for qRT-PCR for gene expression analysis.

Dam-LmnB1 expression line generation

Cloning strategy

To generate a Dam-LmnB1 expression construct, we inserted Dam-LmnB1 into the *Sp3* locus targeting plasmid Sp3-tetO Neo (MB29). This plasmid contains a doxycycline-inducible promoter, as well as an rtTA transgene. We further added an FKBP-V degradation tag to allow for tighter temporal control.

Fragment generation

A Dam-LmnB1 fragment without overhangs was PCR amplified from the plasmid SdV3 p_CCL_PGK-HA-AID-Dam-V5mLmnb1 using primers (table …). Then, overhangs to facilitate Gibson assembly were added to the Dam-LmnB1 fragment using primers MB122 and MB110. Gel extraction was subsequently performed using the NucleoSpin Gel and PCR Clean-up Kit (Macherey-Nagel, 740609.250).

The FKBP-V tag was amplified from pHV1_G9a_FKBP_129_P2A_HygR using primers MB119 and MB120 and isolated by gel extraction. To the FKBP-V tag, a fragment containing a Kozak sequence, and an HA tag (MB118) was added with an 8-cycle two-step PCR of 98ºC-66ºC. In the same tube Gibson overhangs were then added to the fragment using primers MB93 and MB121. Gel extraction on a 2% agarose gel was then performed

The PCR mix per single reaction was 8 µl of HF buffer, 0.8 µl of 10 mM dNTPs, 1 µl of 10 µM primer, 1 µl of plasmid (~100 ng), 0.4 µl of Phusion polymerase and 26.8 µl of H_2O.

Name	Sequence (5'-3')
MB122	CGATGTGGAGCTTCTAAAACTGGAAATGAAGAAAAATCGCGCTTTTTTGA
MB110	GATGGGGGATCCCTTCGCTAGGTTTTCACATAATGGCACAGCTTTTATTG
MB119	GGAGTGCAGGTGGAAACCATCTC
MB120	TTCCAGTTTTAGAAGCTCCACATCGAAGA
MB118	CCGCCATGGGCTACCCATACGATGTTCCTGACTATGCGGGATCCGGAGTGC AGGTGGAAACCATCTCCCCAGGAGACGG
MB93	CGGCCATCACAAGTTTGTACAGTTTCCGCCATGGGCTACCCATACGATGT
MB121	TCAAAAAAGCGCGATTTTTCTTCATTTCCAGTTTTAGAAGCTCCACATCGAAG A

Table 2. List of primers for gibson assembly.

Gibson assembly

The fragments were assembled using a two insert Gibson reaction (50 ng vector : each insert = 1 : 2 molarity) TheSp3-rtTA TetO Neo backbone was linearized using PmeI and FKBP + Dam-LmnB1 DNA inserts with overlapping ends added. First, a 30 minute incubation at 50ºC containing a home-made Gibson master mix with 5' exonuclease, DNA polymerase, DNA ligase and the vector with both inserts was done in a total volume of 10 µl. Second, the mix was diluted with 20 µl of H_2O. Then, transformation was done using 10 µl NEB 10-β with 2 µl of the diluted mix. The transformation mix was incubated for 30 minutes on ice. The heat shock was performed for 45 seconds at 42ºC and 2 minutes on ice. Finally, 300 µl of SOC Outgrowth Medium (NEB, B9020S) was added to the sample and incubated for 1 hour at 37ºC in agitation. Ultimately, the transformation mix was plated on LB petri dishes with Kanamycin and ampicillin and incubated overnight at 37ºC.

Plasmid Amplification and Verification

Single colonies were picked and incubated overnight at 37ºC under kanamycin and ampicillin selection in 3 ml LB. Plasmid DNA was extracted using PureLink Quick Plasmid Miniprep Kit (Thermofisher Scientific, K210011).
Midi prep Plasmid isolation protocol was followed using NucleoBond XtraMidi (Macherey-Nagel, 740410.50)
Control digests were done using restriction enzymes EcoRV and XhoI (2 µl CutSmart buffer, 0.25 µl restriction enzyme, 5 µl DNA, 12.5 µl H_2O). Sanger Sequencing results confirmed a successful incorporation of the Dam-Lmnb1 insert into the vector.

Dam-Lmnb1 Integration in IB10 Mouse ES Cells

Nucleofection was performed using the LONZA P3 Primary Cell 4D-Nucleofector® X Kit L (V4XP-3024) with Amaxa 4D Nucleofector machine (CG-104 program**)**. The transfection mix included 5 µg of gRNA expression plasmid P225-Cas9-2A-GFP Sp3 (Nr. 11) and 3 µg of targeting vector Sp3-rtTA TetO Neo dTAG Dam-Lmnb1. $2x10^6$ cells were transfected. Cells were selected with 300 µg/ml G418 for 7 days in mESC medium on gelatin-coated plates. Subsequently, single clones were picked and expanded.

Verification of Integration Using qRT-PCR

To verify integration of Dam-Lmnb1 into IB10 (hereby called IB10-dDL), clones were screened by qRT-PCR for Dam and rtTA.
First, RNA was isolated from expanded single clones. Second, RNA was reverse transcribed into cDNA using 10 µl of 2x RT Buffer Mix, 1 µl of 20x RT Enzyme Mix and 9 µl of RNA. 10 µl cDNA were then diluted with 90 µl H_2O.
qRT-PCR was performed using the PowerUp™ SYBR™ Green Master Mix following the manufacturer instructions. 5 µl of PowerUp™ SYBR™ Green Master Mix, 0.2 µl of 10 µM Primer mix (forward and reverse primers), 2.8 µl of H_2O and 2µl of diluted cDNA were mixed.

Name	Sequence (5'-3')
MB 127 Dam_q_fw	TCAGTTCCGCGAAGAGTTCAA
MB 128 Dam_q_rv	CCATGCTATCGGCGTAAGACT
MB 90 rtTA_q_F1	CTACCACCGATTCTATGCCCC
MB 91 rtTA_q_R1	CGCTTTCGCACTTTAGCTGTT
MB 24 Gapdh_q_F1	ATGAATACGGCTACAGCAACAGG
MB 25 Gapdh_q_R1	CTCTTGCTCAGTGTCCTTGCTG

Table 3. List of primers for qRT-PCR for integration verification.

Methylation-specific PCR

To verify the functionality of IB10-dDL clones, Dam-specific methylation was measured using methylation-specific PCR.

gDNA extraction was performed using thePromega Wizard Kit (A7953) following the manufacturer's instructions. First, methylated GATCs were digested by DpnI for 30 minutes at 37ºC using 2 µl of CutSmart 10x, 1 µl of DpnI (20 units), 2 µg gDNA, and filled-up with H_20 for a final volume of 20 µl per mix. Next, blunt-end adapters were ligated using T4 ligase for 30 minutes at 25ºC followed by heat inactivation for 20 minutes at 65ºC. Each sample mix contained 1 µl dsAdapter (50 µM), 2 µl T4 buffer, 0.5 µl T4 Ligase, 5 µl DpnI gDNA and 11.5 µl H_2O for a final volume of 40 µl per mix. Subsequently, a 0.8 V bead clean-up was performed. Finally, 14 cycle MethylPCR was done using 528 DamID_NNNN_DpnI_PCR NNNNGTGGTCGCGGCCGAGGATC, and double stranded adapters sequence CTAATACGACTCACTATAGGGCAGCGTGGTCGCGGCCGAGGA and TCCTCGGCCGCG. The PCR mix per single reaction was 4 µl MyTag buffer, 0.2 µl MyTag pol2, 2.5 µl 528 primer, 50 ng gDNA (DpnI and Adapter ligated) and 5.3 µl H_2O.

Results

Protocol optimizations

To generate mouse retinal organoids, we followed a published protocol by the Karl lab (Völkner et al., 2016). This protocol can be divided into two stages, pre-culture and organoid culture. Pre-culture consists of mES cell culture to ensure that cells are competent for differentiation into mouse retinal organoids. Organoid culture phase starts from the aggregation (D0) until the organoid harvesting (D30-40). There are major aspects to consider during this phase. Those being membrane matrix addition needed for the 3D structure development, transfer to bacterial dishes and the trisection to increase the overall retina yield of the organoid.

However, details regarding the mouse ES cell pre-culture were insufficient for us. For the organoid culture in general, we followed Karl lab protocol and minor optimizations were made. We therefore optimized multiple steps to achieve a more robust protocol.

Pre-culture optimizations

Importance of PD treatment in cell differentiation during pre-culture

ESCs are self-renewing, pluripotent cells, having the ability to differentiate into cells of all three germ layers (Tsumura et al., 2006). Usually ESCs are cultured in Serum/LIF medium. However, the Karl lab protocol further adds PD0325901 (PD) to the Serum/LIF medium during the pre-culture. While the reason for this is not given in the protocol, we speculate that adding PD is beneficial for promoting neuroectodermal precursor differentiation (Yu et al., 2018).

Consequently, we wanted to determine if the addition of PD during the pre-culture is indeed necessary and assess the duration of its treatment. Thus, for this experiment a standard protocol was followed and mESCs were either cultured without PD treatment or with one day of PD treatment added at D-1. After aggregation on D0, mouse retinal organoids were cultured.

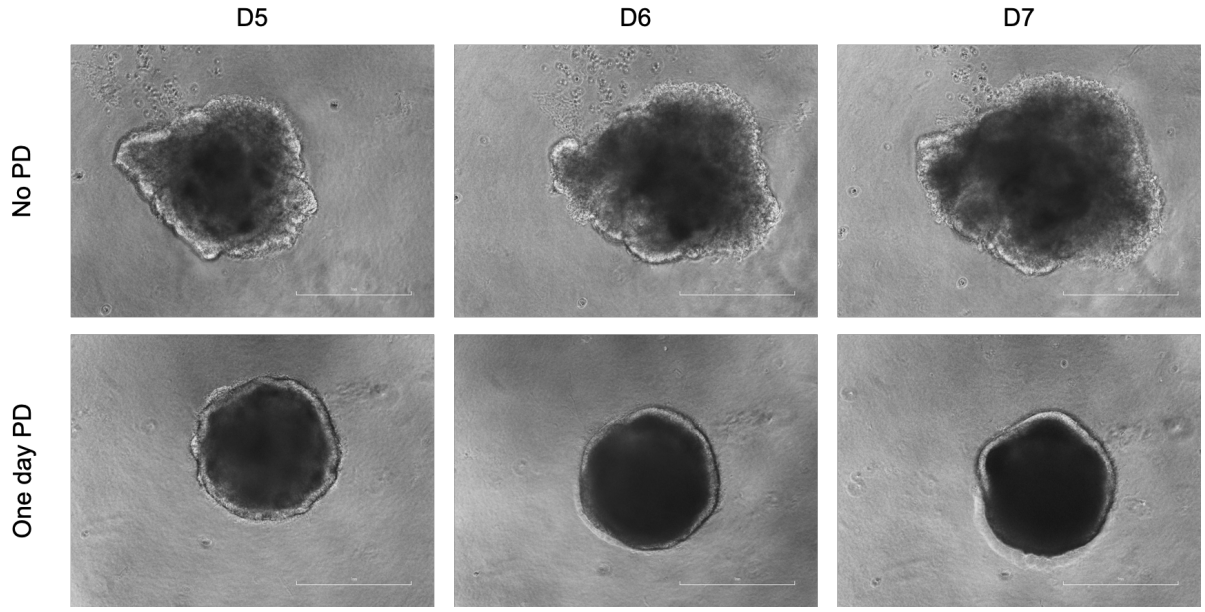

Figure 3. Brightfield images of mouse retinal organoids without PD (No PD) and one day PD treatment through D5-D7. Taken at 20x magnification. Scale bar 1mm.

We visually assessed mROs during the early stages of differentiation, from day 5 to day 7, when organoids are expected to show a visible neuroepithelium layer encompassing the edge of the whole organoid. On one hand, as seen in figure 3. organoids with PD treatment formed a clear and continuous neuroepithelium. On the other hand, organoids originating from ESC without PD treatment did not develop the expected layer. In some organoids the neuroepithelium layer was present but was not continuous and located in small regions only. To conclude, PD treatment is essential for organoids to develop the continuous neuroepithelium layer needed for further differentiation to the photoreceptor layer.

Extended PD treatment is beneficial

Since showing the importance of adding PD during mESC pre-culture (Figure 3), I further wanted to assess whether the duration of the PD treatment was important.

For this end I followed the experimental set-up from before, but now compared treating cells either for one day or for 2 days with PD before aggregation.

When comparing the two conditions, inspection of brightfield images showed highly similar organoids during the early days D4-D6 (Figure 4). This pattern continued through further days D12-D14. Even though we noticed that extended treatment is beneficial, no other major conclusions could be extracted from the brightfield images.

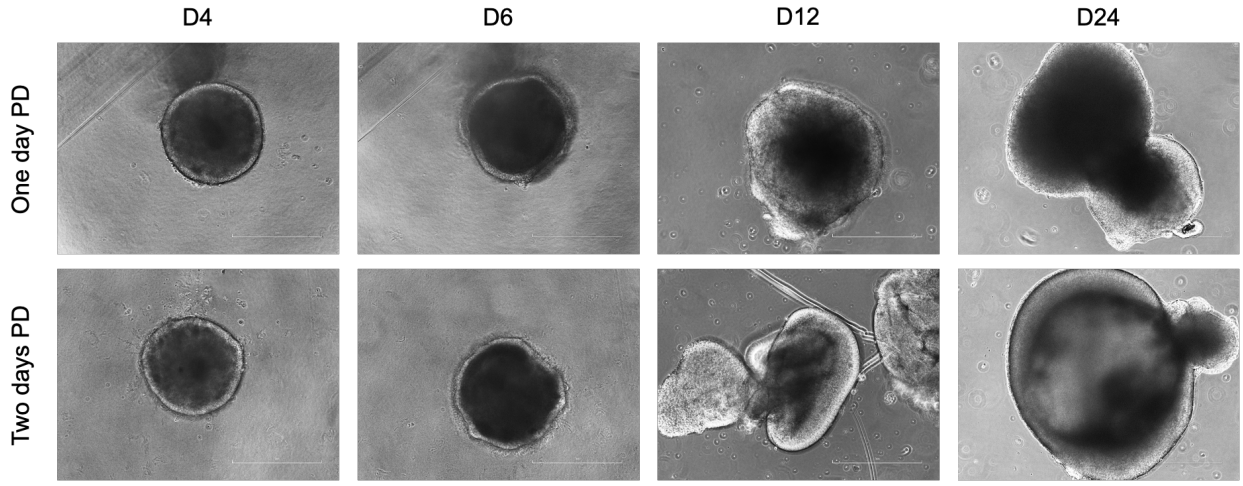

Figure 4. Brightfield images of mouse retinal organoids with one day PD and two days PD treatment (PD2) through D4, D6, D12 and D24. Taken at 20x magnification. Scale bar 1mm.

To further explore for differences in the organoid structure i.e different layer distribution between the two comparisons of PD treatment. Hematoxylin and eosin stainings were performed of D25 organoids. Both conditions had the desired traits, i.e retinal surface with defined layers including the inner and outer photoreceptors segments. Outer nuclear layer (ONL) followed by the outer plexiform layer (OPL) and inner nuclear layer (INL). However, H&E images of two days PD treatment tend to present a broader retina surface compared to the one day PD treatment.

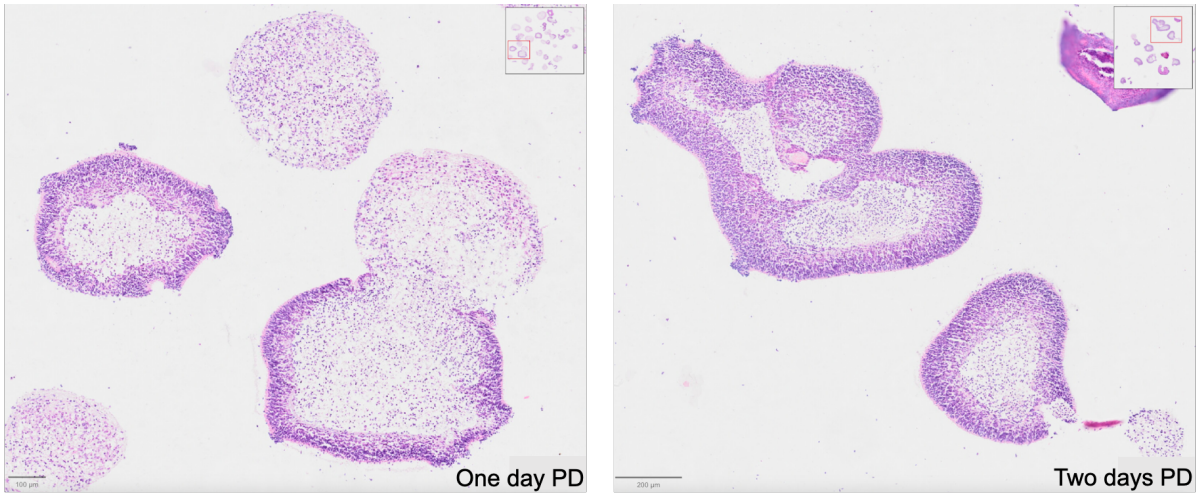

Figure 5. Hematoxylin and eosin staining images of D25 mRO one day PD treatment (left) and two days PD treatment (right). Taken at 20x magnification. Scale bar 100µm (left) 200µm (right).

In conclusion, no major differences were observed between one day PD and two days PD. However, we note a trend for extended PD treatment to show more mature structures, which should be quantified in the future. Therefore, two days of PD treatment will be used henceforth if not stated otherwise.

Confluency and seeding density of mESCs

In the course of experiments assessing the importance of PD, I had observed that during the initial stages of mESC pre-culture, a considerable amount of differentiating cells was visible when confluency was low. I therefore argued that a higher confluence could be beneficial for mRO differentiation, as it would lead to a purer starting mESC culture. For that reason, I tested different confluencies during the pre-culture of mESCs.

To determine the confluency and seeding density of mESCs, we followed the standard protocol and cultured mESCs as usual except on D-1, when apart from adding PD, cells were split at multiple seeding densities ($2x10^5$ cells/well, $4x10^5$ cells/well, $6x10^5$ cells/well and $8x10^5$ cells/well of cell solution). Then on D0 aggregation was performed.

Figure 6. shows brightfield images of the IB10 cell line taken on D0 before the aggregation. Seeding densities from left to right: $2x10^5$ cells/well, $4x10^5$ cells/well, $6x10^5$ cells/well and $8x10^5$ cells/well. At $6x10^5$ cells/well,, we observe 80% confluency (an optimal percentage for numerous protocols) and lower amounts of differentiating cells.

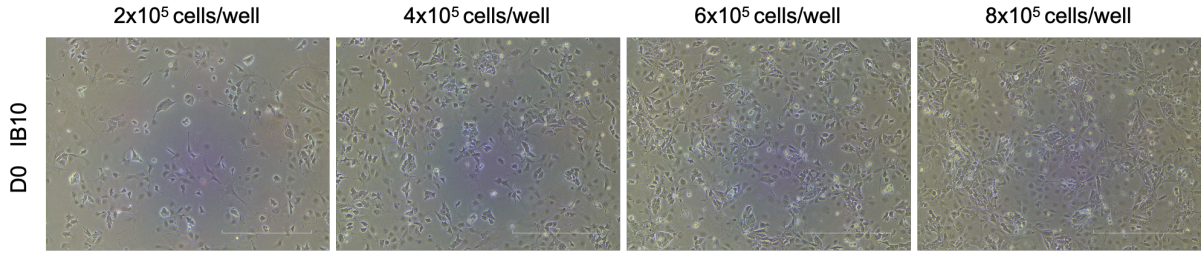

Figure 6. Brightfield images of different seeding densities of D0 IB10 cells. Taken at 20x magnification. Scale bar 1mm.

Furthermore, when assessing mRO structure after 6 days of differentiation (Figure 7), I observed a thicker neuroepithelial rim as well as rounder organoids from higher seeding densities ($6x10^5$ and $8x10^5$ cells/well) compared to lower density ones.

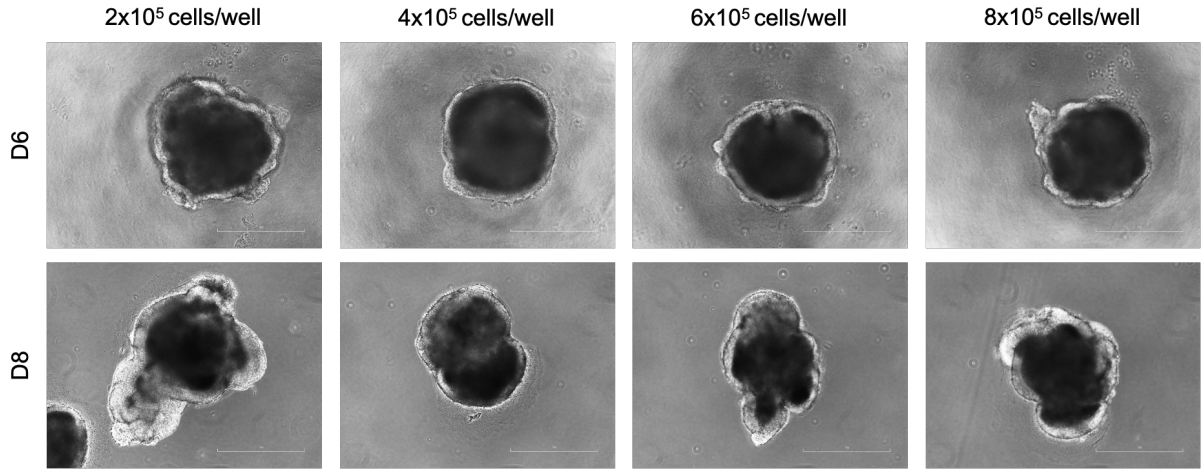

Figure 7. Brightfield images of mROs from different pre-culture seeding densities at D6 (upper row) and D8 (lower row). Taken at 20x magnification. Scale bar 1mm.

To conclude, mRO differentiation is improved by optimizing mESC seeding density to $6x10^5$ - $8x10^5$ cells/well at D-1.

Removal of differentiating cells via depletion step

As discussed before, during mESCs pre-culture differentiating cells were observed. To decrease the amount of differentiating cells, a depletion step was added on the day of aggregation (D0). This step consisted of a 40 minute incubation on a gelatin coated 15 cm plate. As differentiating cells tend to attach to the plate faster than mESCs, the supernatant will be enriched for mESCs.

Consequently, to determine the importance of the depletion step, we followed the standard protocol and one day of mESC PD treatment. Then on D0 aggregation was performed with one condition following the regular aggregation protocol (called No depletion condition) and the other condition following the same protocol plus an extra depletion step (called Depletion condition). After that organoids were cultured following the Karl lab protocol.

To explore if the additional depletion step has an effect on the organoid structure overtime, hematoxylin and eosin stainings were performed at day 25.

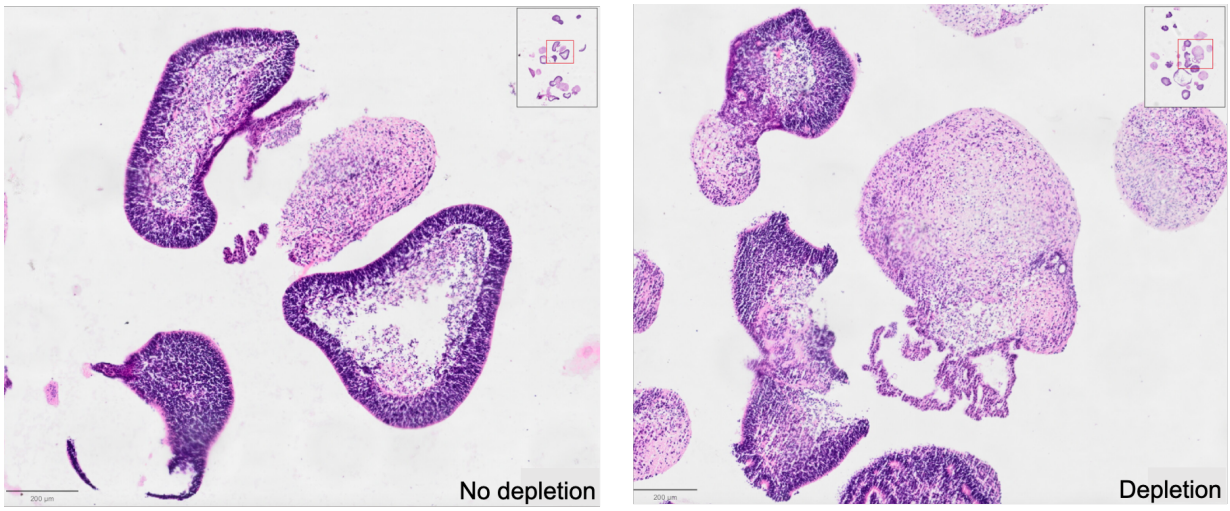

Figure 8. Hematoxylin and eosin staining images of D25 mRO without the additional depletion step (left) and with depletion step (right). Taken at 20x magnification. Scale bar 200µm.

Organoid culture optimizations

Geltrex as a substitute to Matrigel

Due to limited availability and relatively high cost of Matrigel™, we wanted to test Geltrex™ as a more available and cheaper alternative. Additionally, Geltrex™ is a more defined product regarding protein concentration from batch-to-batch in comparison to Matrigel™ (Gargotti et al., 2018).

On one hand, Matrigel™ is an extracellular matrix (ECM) derived from mouse Engelbreth-Holm-Swarm (EHS) tumors. The major components of Matrigel™ are collagen type IV, laminin, entactin, perlecan and heparan sulfate proteoglycan (Kim et al., 2022). On the other hand, Geltrex™ LDEV-Free Reduced Growth Factor (RGF) Basement Membrane Matrix has the same purpose as Matrigel™. It is a basement membrane matrix extracted from murine

Engelbreth-Holm-Swarm (EHS) tumors. Its major components are laminin, collagen type IV, heparin sulfate proteoglycans and entactin (Gargotti et al., 2018).
To conclude, both Geltrex™ and Matrigel™ are derived from Engelbreth-Holm-Swarm tumors. However, Geltrex™ has a more defined protein concentration. Thus, allowing a higher experimental throughput.

To explore for differences in the organoid structure between Matrigel™ and Geltrex™, we followed the standard protocol with two days of mESC PD treatment, followed by addition of either Matrigel™ or Geltrex™ on D1 of organoid culture. Brightfield microscopy showed no major differences between the two types of basement membrane matrix at different timepoints.

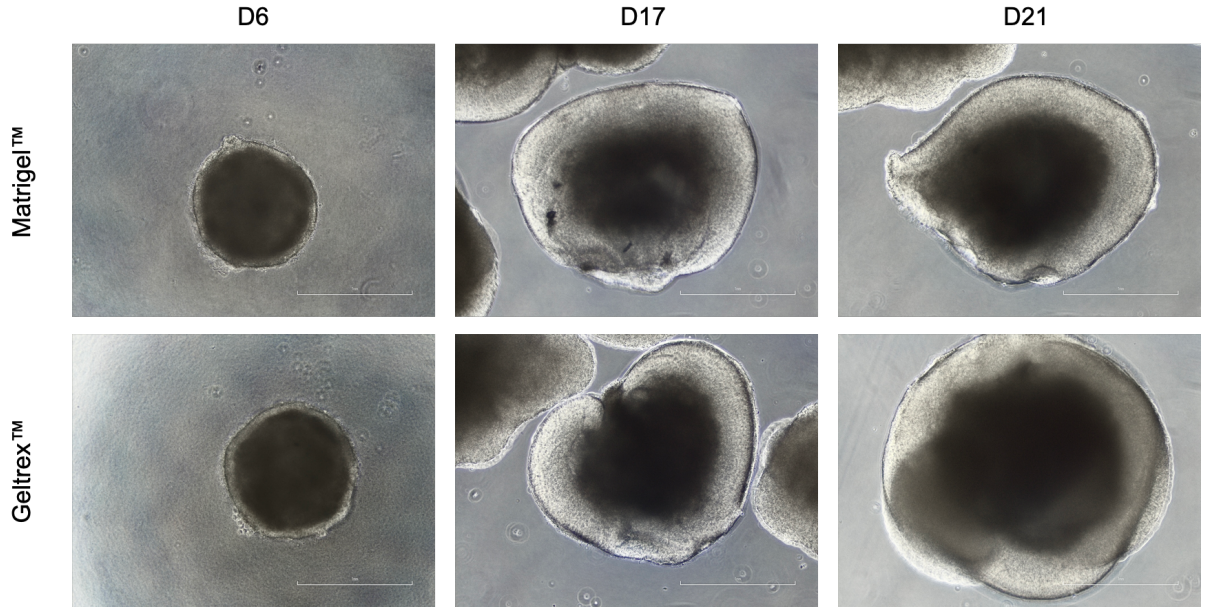

Figure 9. Brightfield images of mRO with Matrigel™ (upper row) and Geltrex™ (lower row) at D6, D17 and D21 of organoid culture. Taken at 20x magnification. Scale bar 1mm.

Furthermore, to gain more detailed insights if the structure of the organoids varies between Matrigel™ and Geltrex™. Hematoxylin and eosin staining were performed on D25. However, no major differences were observed when comparing the retinal rim thickness and the layers composition between both conditions.

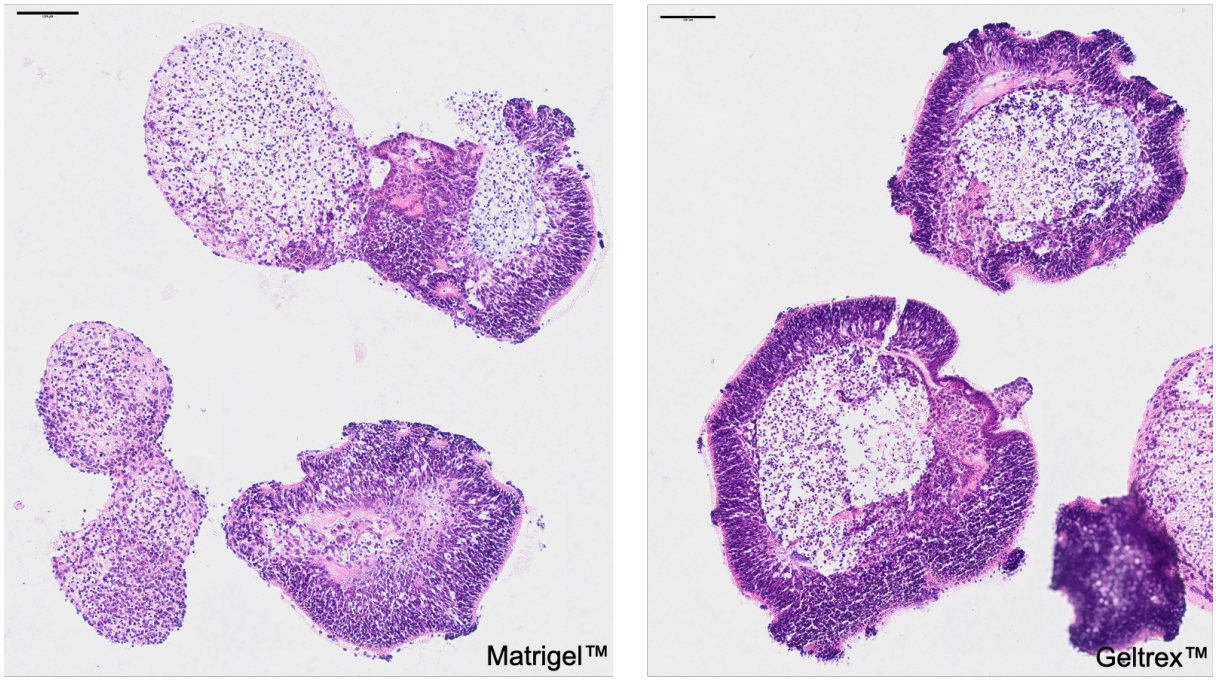

Figure 10. Hematoxylin and eosin staining images of mRO on D25 organoids of both Matrigel™ (left) and Geltrex™ (right) conditions. Taken at 20x magnification. Scale bar 100µm.

To summarize, Geltrex™ is a suitable substitute for Matrigel™ since no major differences were observed.

Oxygen levels comparison shows no major differences

The Karl-lab protocol cultures retinal organoids from D7 onwards under 40% oxygen. However, until now, our organoids were cultured routinely at 20% oxygen. To gain insights if this increased percentage of oxygen will affect the organoid structure in terms of thickness and richness of the neuroepithelium rim, we wanted to compare mRO culture under these two oxygen conditions.

The standard protocol of mESCs pre-culture was followed. Both conditions remained under 20% oxygen until D7. Then, part of the organoids were transferred to 40% oxygen until D25.

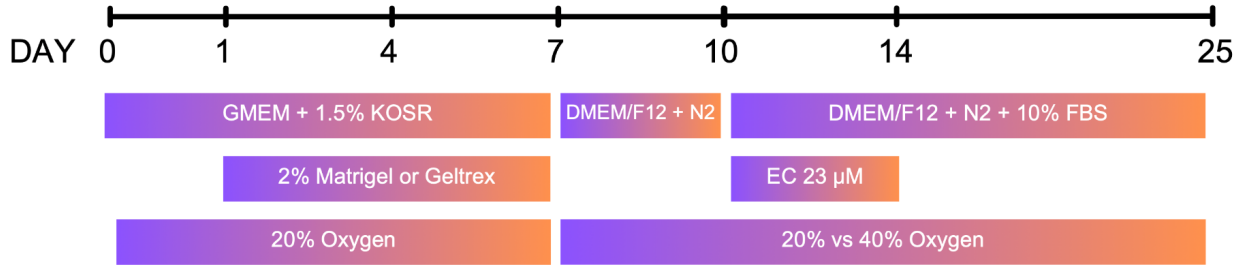

Figure 11. Representative diagram of the experimental set-up, comparing culture of mROs in 20% and 40% oxygen. From D0 to D25 of organoid culture.

To explore variations of the organoid structure at 20% and 40% oxygen overtime, Hematoxylin and eosin stains were performed at D25.

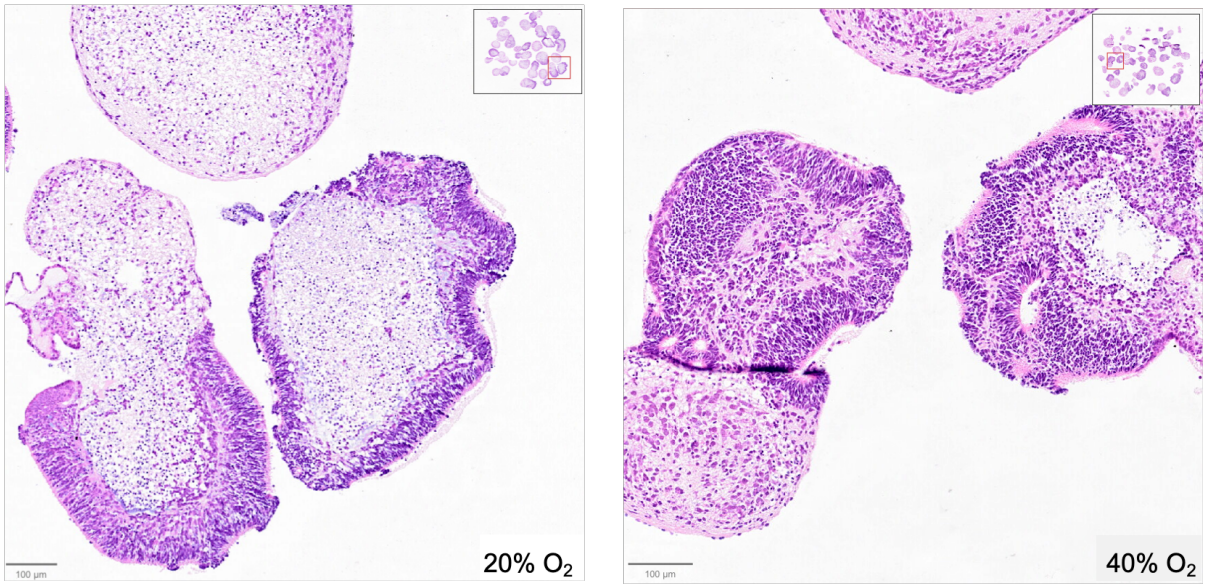

Figure 12. Hematoxylin and eosin staining images of mRO on D25 organoids of 20% oxygen (left) and 40% oxygen levels (right). Taken at 20x magnification. Scale bar 100µm.

When quantifying retinal organoid efficiency, in other words the percentage of organoids harboring the characteristic retinal layers, we found a high percentage of around 60% in both conditions (Figure 13 A). Moreover, when further measuring the percentage of retina surface, the area occupied by retinal layers in each mRO, an average of 10% were found to be occupied in both conditions (Figure 13 B). To conclude, this data shows no major differences for the culture of mROs in 20% and 40% oxygen. However, we can't exclude that differences might arise after D25 of differentiation or might be observed at the molecular level.

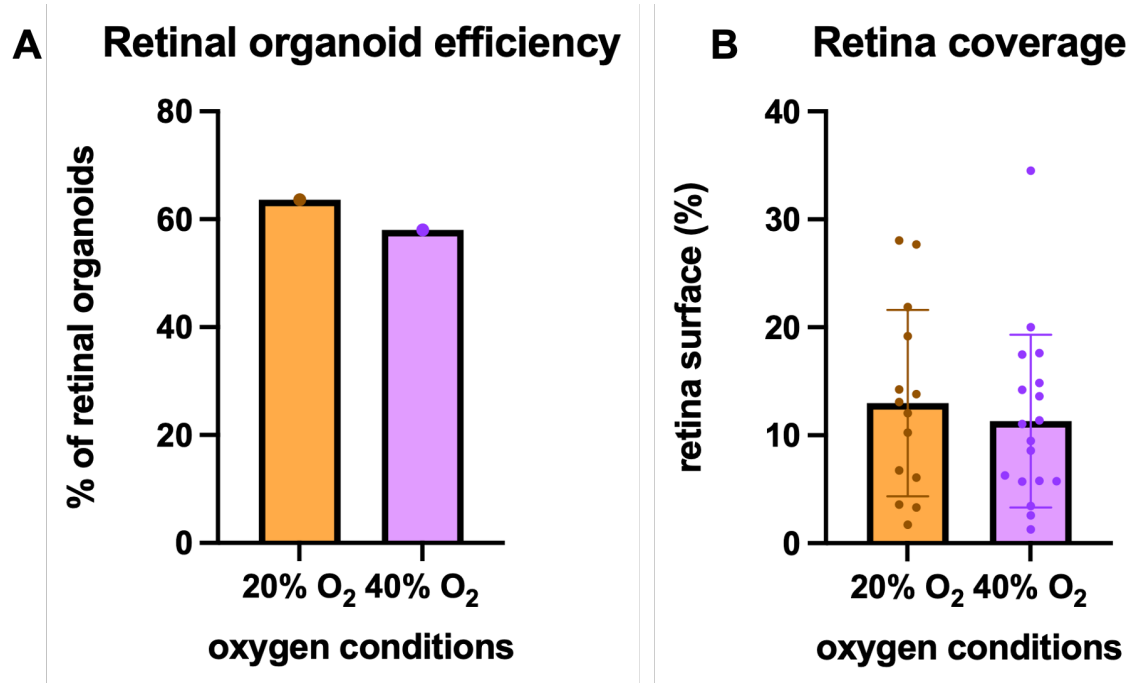

Figure 13. Comparing culture of mROs in 20% and 40% oxygen. **A**. Retinal organoid efficiency based on the percentage of retinal organoids compared to the total amount of retinal and non-retinal organoids. D25 mROs are compared at 20% or 40% oxygen levels. **B**. Retina coverage based on the percentage of retinal surface comparing 20% and 40% oxygen conditions at D25. Each dot represents one retinal organoid.

IB10 over F1ES cell line comparison

Once the protocol was optimized, we wanted to compare mRO competence for IB10 cells versus F1ES cells. Specifically, we aimed to assess changes in morphology and marker gene expressions of organoids derived from F1ES and IB10 mESCs.
I followed the optimized protocol with pre-culture, consisting of two days of PD treatment.

Even though we used our optimized protocol for the generation of mROs from F1ES cells, we failed to generate retinal organoids. We expected F1ES mRO to form similar retinal structures as IB10 mROs. However, F1ES did not yield retinal organoids (Figure 14).

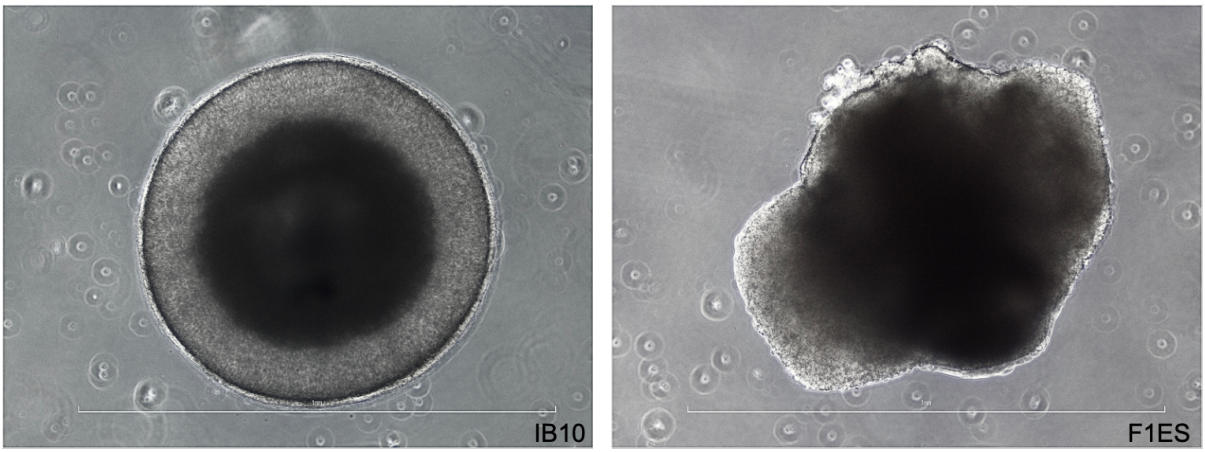

Figure 14. Brightfield images of mRO from IB10 cells (left) and mRO from F1ES cells (right) at D20. Taken at 20x magnification. Scale bar 1mm.

Moreover, to gain a deeper insight into the layer structure of the organoids, hematoxylin and eosin stainings were performed on IB10 and F1ES mROs at D35. Whereas IB10 mRO had a defined layer distribution in accordance with the retinal organoids i.e photoreceptor layer, outer nuclear layer, and outer plexiform layer, F1ES mROs did not form a retina-like structure with any of the retinal organoid layers.

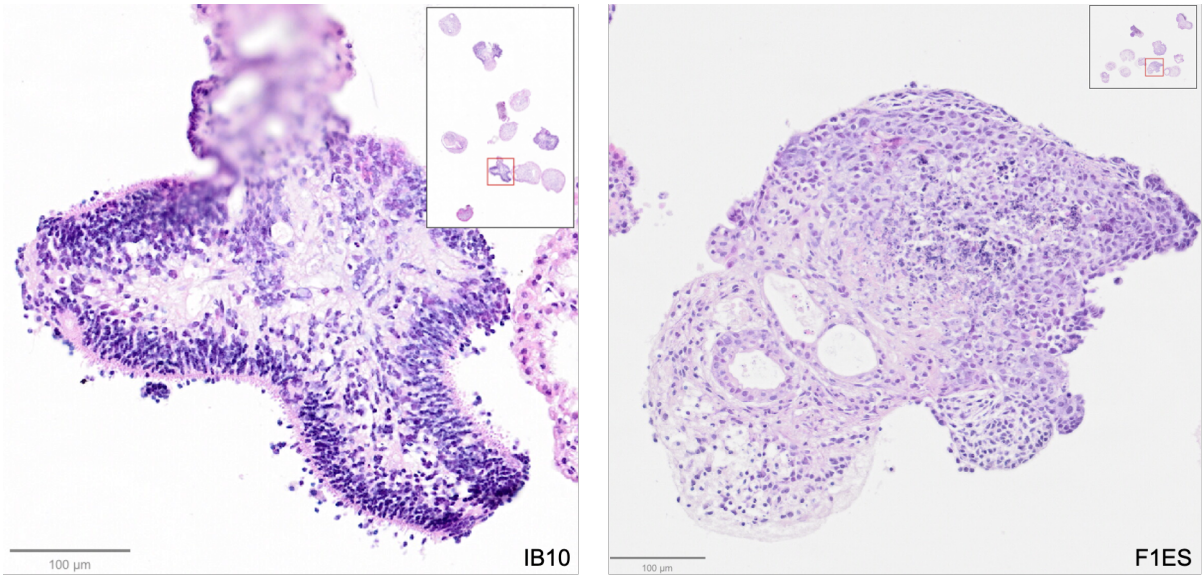

Figure 15. Hematoxylin and eosin staining images of D35 mRO from IB10 cells (left) and F1ES cells (right). Taken at 20x magnification. Scale bar 100µm.

Apart from the visual observations, to validate the effectiveness of the protocol optimizations on the retinal organoids, qRT-PCR was performed on IB10 and F1ES mROs using early and late photoreceptor (*Crx*, *Nrl*, *Rcvrn*, *Rho* and *Arr3*), progenitor (*Vsx2*, *Sox9* and *Pax6*) and stemness markers (*Neurod6*). Marker genes were taken from (Völkner et al., 2016).

The photoreceptor markers are classified in two subgroups: Early photoreceptors markers (*Crx* and *Nrl*), expected to increase from D15 onwards and mature photoreceptors markers (*Rcvrn*, *Rho* and *Arr3*), expected to increase later.
Indeed, the earliest regulator of photoreceptor genesis *Crx* increased its expression after D15, reaching a maximum at D25. After this, levels decreased slowly. Moreover, *Nrl*, known as the earliest postmitotic photoreceptor marker, showed a similar expression pattern.

From D20 on, we expected to see an increase of mature photoreceptor expression. Consequently, *Rcvrn* expression levels increased after D20, reaching its maximum by D30. *Rho,* a marker for rod cells, started its expression after D20 with an exponential increase until D35. *Arr3,* a marker for cones, started its expression only from D20.

The progenitor markers (*Vsx2*, *Sox9* and *Pax6)*, were expected to show expression during early and late phases of retinogenesis. *Vsx2,* known to be the earliest specific marker of retinal progenitors specially in bipolar cells, reached its expression maximum by D20 and continued until D30, then it started to decrease. *Sox9* expression levels were already high by D15., then decreased by D25 and increased reaching its maximum by D35. *Pax6* expression levels exponentially decreased since D15.

In regard to the remaining expression marker, *Neurod6,* for interneurons. Its levels decreased after D15 and on D30 slightly increased.

In contrast, aggregates from the F1ES cells only showed expression of *Sox9* and *Neurod6* with increased values after D15 and at the same level until D30. Therefore, F1ES cells did not meet the morphological criteria of retinal organoid formation nor the gene expression patterns.

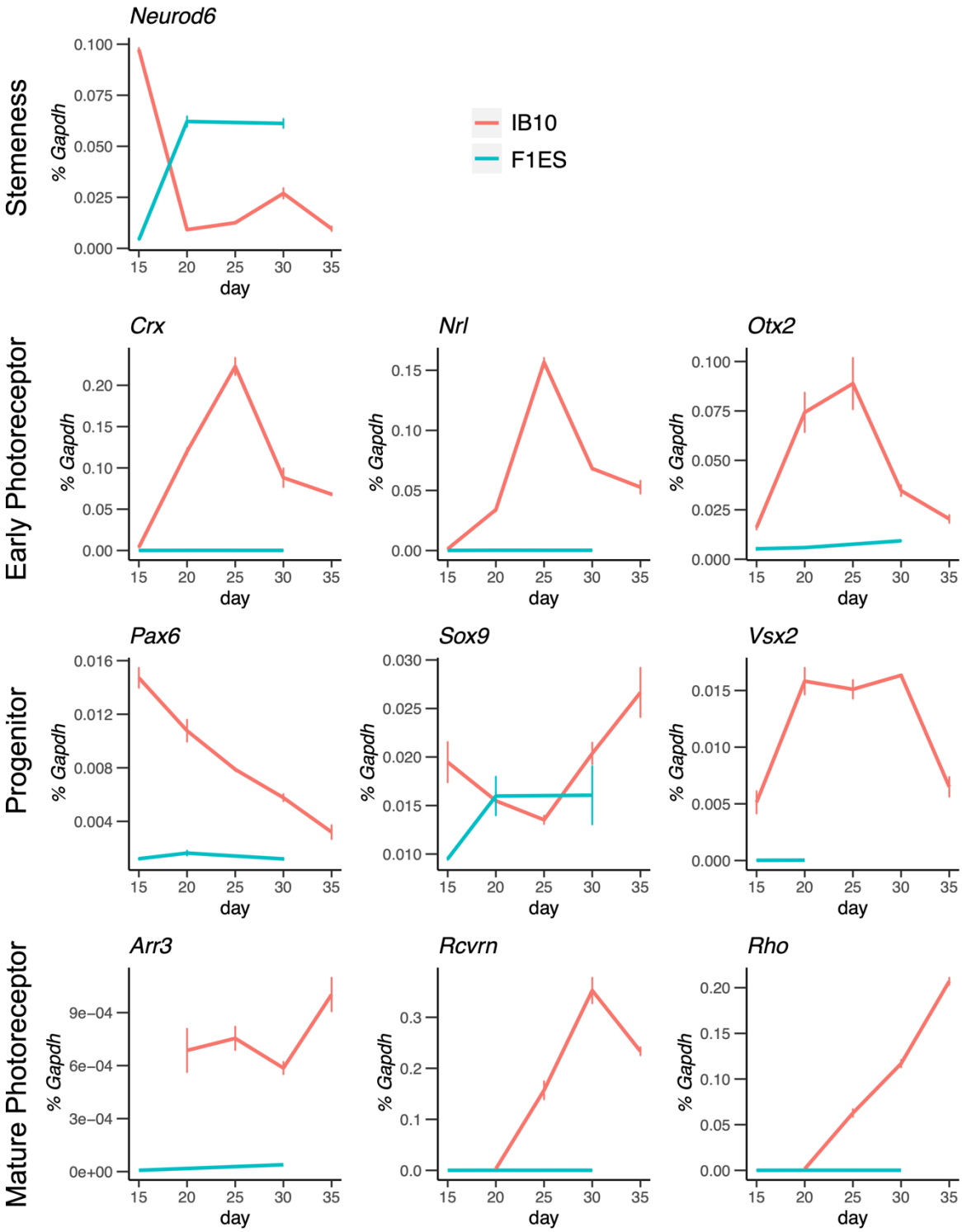

Figure 16. qRT-PCR of IB10 and F1ES mROs at different timepoints. Stemness marker used was *Neurod6*. Early photoreceptor markers used were *Crx*, *Nrl*, *Otx2*. Progenitor markers used were *Pax6*, *Sox9* and *Vsx2*. Late photoreceptor markers used were *Arr3*, *Rcvrn*, *Rho*. Normalized to *Gapdh*. n = 1 biological sample. Error bars denote SEM from 3 technical replicates.

Chromatin inversion in late organoids

Through the organoid culture, on D40 mRO samples were fixated and DAPI stained following the standard protocols mentioned at Materials and Methods. DAPI staining was done to assess the nuclear organization of the cells present at the retina layer. More specifically, nuclei organization of rods in comparison to the conventional organization of the rest of cells i.e bipolar cells. Figure 16 shows rod cells (R) already with the inverted organization while the bipolar cells (BP) present a conventional distribution.

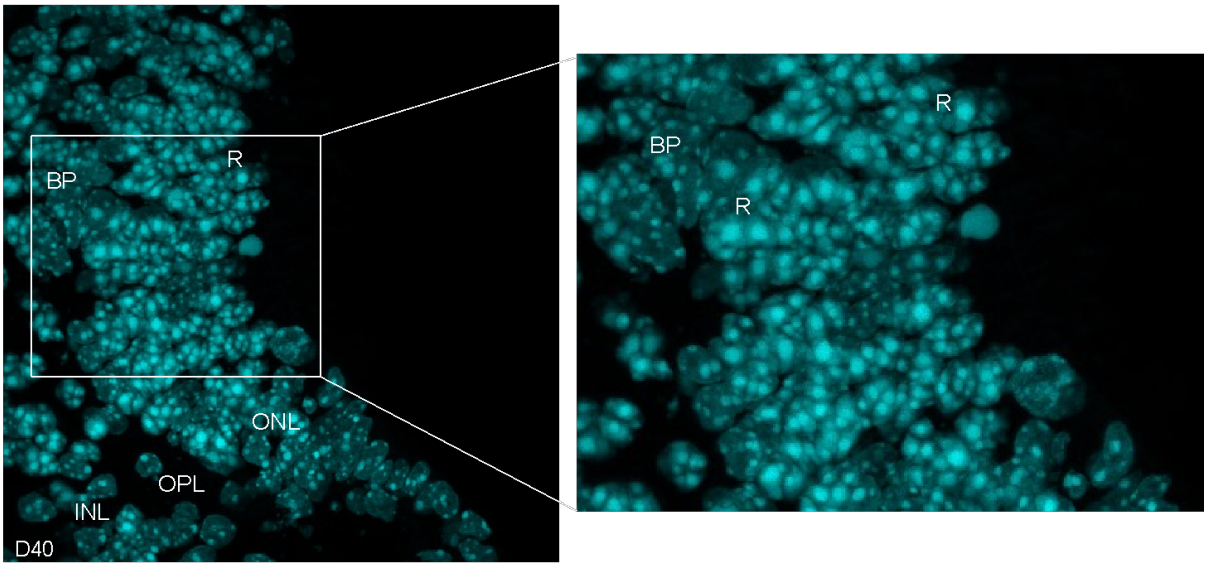

Figure 17. DAPI stained images of D40 mRO from IB10 cells. Bipolar cells (BP), rod cells (R), inner nuclear layer (INL), outer plexiform layer (OPL), outer nuclear layer (ONL) . Taken at 63x magnification.

IB10 Dam-Lmnb1 cell line generation

As shown previously, F1ES cells do not yield mouse retinal organoids even when using our optimized protocol. Since our aim is to study rod inversion in nocturnal mammals, using genome-nuclear lamina interaction as the main read-out, a Dam-Lmnb1 expressing cell line competent for mRO differentiation was needed. We therefore aimed to integrate a Dam-Lmnb1 overexpression vector into IB10 cells, to be able to study genome-nuclear lamina interactions with DamID before, during and after the inversion. The method known as DamID, utilizes a DNA adenine methyltransferase (Dam), to identify DNA regions that interact with a protein of interest fused to it. It is especially helpful for exploring genome-wide interactions between proteins and DNA (Orian et al., 2009). Dam methylates the adenines of the GATC motif in close proximity to the protein-DNA binding sites (Greil et al., 2006). Thus, in our case it serves to label DNA in proximity to laminB1 to map lamina-associated-domains (LADs).

Dam-Lmnb1 Expression Vector Design and Cloning

The cloning strategy to generate a Dam-LmnB1 expression construct was to insert Dam-LmnB1 into the *Sp3* locus targeting plasmid Sp3-tetO Neo (MB29). Here, expression of the Dam-Lmnb1 transgene is driven by a doxycycline-inducible tetO promoter with an rtTA

transactivator in the same vector. Furthermore, a FKBP-V degradation tag was added to potentially control the protein activity using dTAG. When dTAG is added it induces the degradation of Dam-Lmnb1 and could help to eliminate background signal. Therefore, the combination of these two factors contributes to tighter temporal control
To integrate the Dam-Lmnb1 insert and FKBP-V tag into the Sp3-tetO Neo plasmid, a two insert Gibson Assembly was performed.

Figure 18. Schematic overview of the *Sp3* targeting Dam-LmnB1 expression vector.

To validate correct integration of the Dam-Lmnb1 insert into *Sp3* a restriction digest was performed using restriction enzymes EcoRV and XhoI. This showed that all clones presented the insert and backbone fragments with the right length.

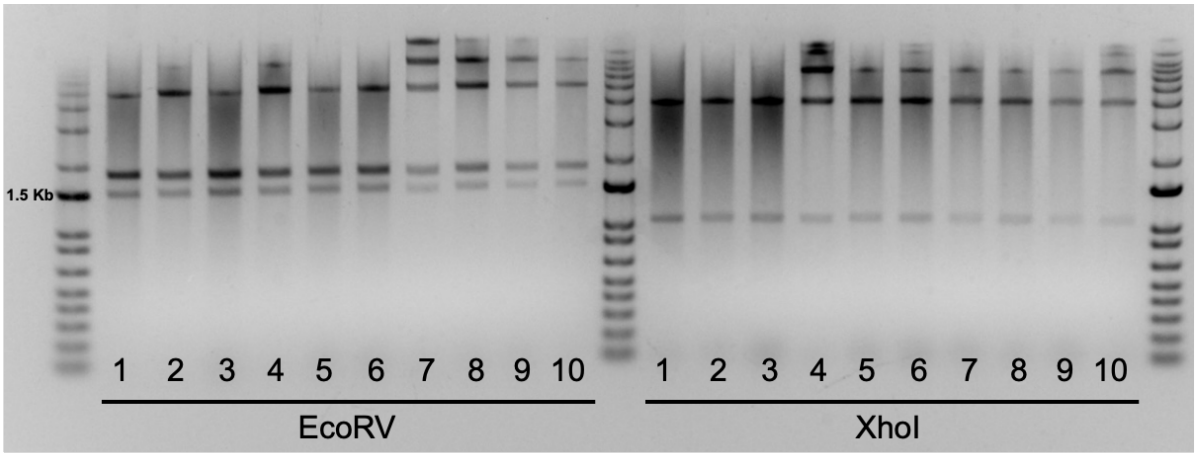

Figure 19. EcoRV and XhoI restriction digest to verify the correct integration of the Dam-Lmnb1 insert into the *Sp3* targeting plasmid.

Additionally, to validate if the insert was ligated into the right position Sanger Sequencing was performed. Results came back positive, Dam-Lmnb1 was correctly inserted at the specific region of the *Sp3* vector.

Dam-Lmnb1 Integration into IB10 mESCs

After successfully cloning of the Dam-LmnB1 expression vector, I nucleofected the vector and Sp3 targeting gRNA and Cas9 into IB10 mESCs. Because other common screening strategies like PCR, weren't suitable due to the large homology arms of the insert. Dam-Lmnb1 integration into IB10 cells (IB10_dDL), was quantified using the expression levels of Dam and the rtTA transactivator in all clones. Nucleofected IB10_dDL had an 8 hours of incubation with doxycycline to induce Dam-Lmnb1 transgene expression. Then RNA was isolated and reverse transcribed to cDNA for subsequent quantitative RT-PCR (qRT-PCR). Following, standard qRT-PCR was performed to measure Dam and rtTA expression levels in each clone.
I found that all clones, except for #16, had expressions of both Dam and rtTA. Clones 1, 9 and 13 had the highest expression of Dam and rtTA. Moreover, Dam and rtTA expression was correlated, indicating full-length integration in all plasmids

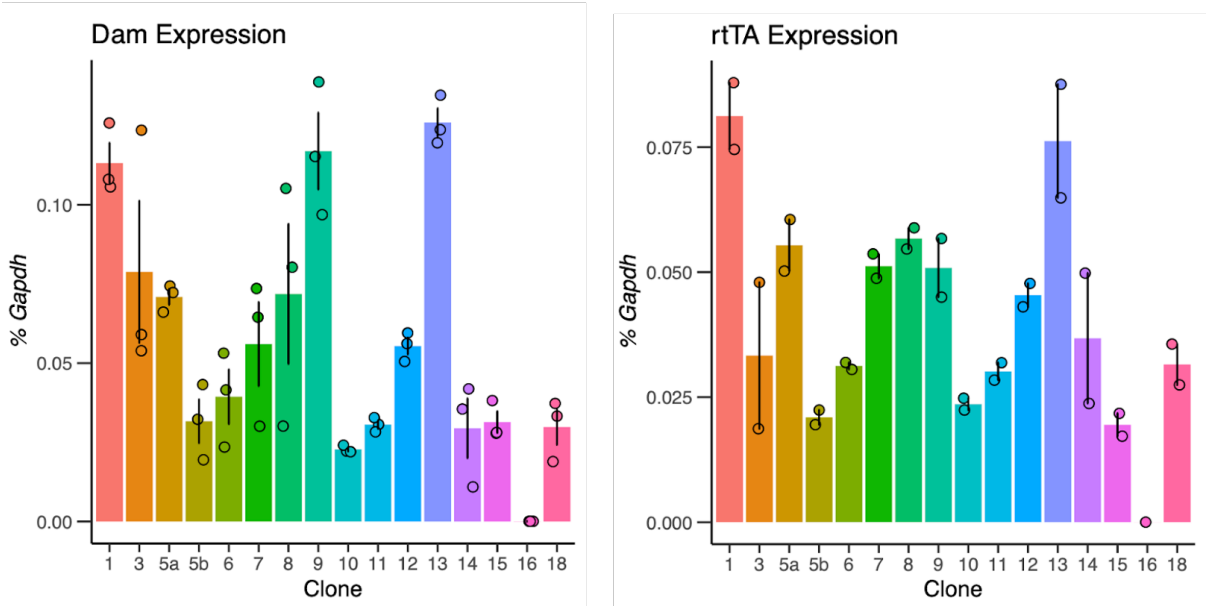

Figure 20. qRT-PCR to measure Dam and rtTA expression for all 18 clones. Normalized to *Gapdh*. n = 1 biological sample. Error bars denote SEM from 3 technical replicates shown as points.

MethylPCR for Dam-LmnB1 induction

To validate that our Tet-On system was functional, as well as to determine the optimal induction time for Dam-Lmnb1, a MethylPCR was done for 3 clones, #1, #9 and #13, which showed the highest expression of Dam and rtTA. To this end, cells were cultured with dTAG (500nM) to eliminate any background. Then, samples were taken at 0 hours, 4 hours of doxycycline only and doxycycline with dTAG (2 µM) induction, 8 hours of doxycycline only and doxycycline with dTAG induction. The MethylPCR involves a gDNA extraction followed by DpnI digestion to cut all the GATC methylated by Dam. Then T4 adapter ligation was performed to add adapters to the cut DNA fragments and finally adapter ligated fragments were amplified using PCR. This technique allowed us to determine if there was Dam methylation upon addition of doxycycline, the intensity of the methylation levels in all clones and to validate if dTAG was able to degrade the Dam-Lmnb1 fusion protein.

As shown in figure 21, without the addition of doxycycline no methylation is observed, indicated by a lack of a methyl smear at 0h. However, after four hours of doxycycline induction, the methyl smear was present, indicating successful methylation of GATCs. Moreover, the methylation signal was then increased after eight hours of doxycycline induction. Then we also did inductions with doxycycline and dTAG, to measure if dTAG is able to degrade Dam-Lmnb1. After four hours of doxycycline and dTAG induction clone 1 showed a similar level to the induction without dTAG whereas clones 9 and 13 had less signal, indicating that dTAG was able to degrade Dam-Lmnb1. However, after eight hours, the methylation signal in all three clones was similar for plus and minus dTAG, suggesting that dTAG is only able to degrade lowly-expressed Dam-Lmnb1
In closing, induction by doxycycline was functional, with stronger signal after eight hours. In contrast, dTAG is not able to degrade the transgene when levels are high.

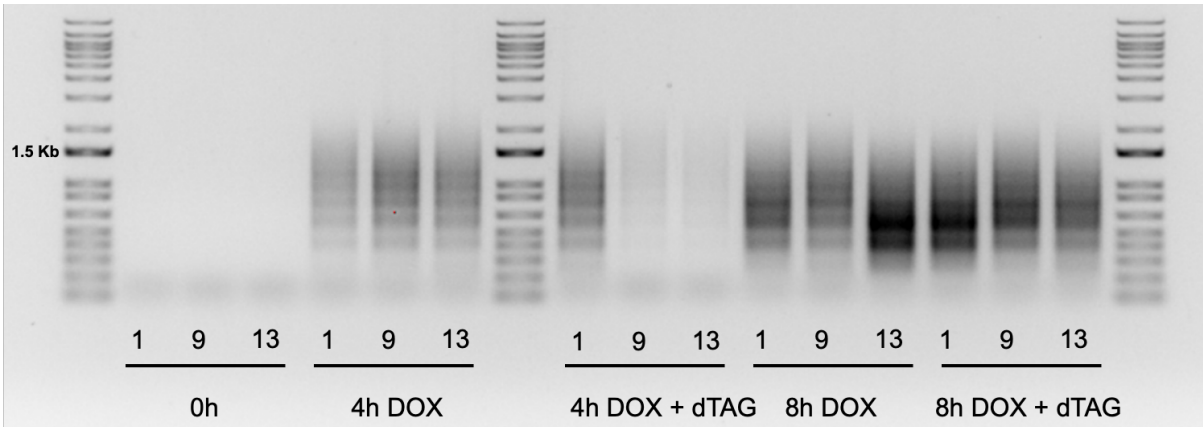

Figure 21. PCR-amplified methylated DNA fragments are shown under various conditions to determine Dam-Lmnb1 induction for clones 1, 9 and 13. Successful methylation is shown by a smear from 200 bp to 2,000 bp. Four and eight hours of doxycycline (DOX) induction, as well as four and eight hours of DOX plus dTAG induction.

Locating methylations in cells by m6A-tracer staining

To further validate that the IB10 Dam-Lmnb1 cell line can be used for studying interactions between the nuclear lamina and the genome, an m6A-tracer staining was performed to localize Dam methylation. This DamID-derived approach called m6A-tracer, tracks the interactions between the NL and genome in single cells by using a truncated form of DpnI without enzymatic activity, fused to GFP (Kind et al., 2013). Methylated GATCs can therefore be bound and visualized. m6A tracer was performed on the IB10 Dam-Lmnb1 cells for lamina associated domain (LAD) validation. Out of 2 cells, one shows m6A staining at the nuclear lamina, indicating methylation of DNA in its proximity.

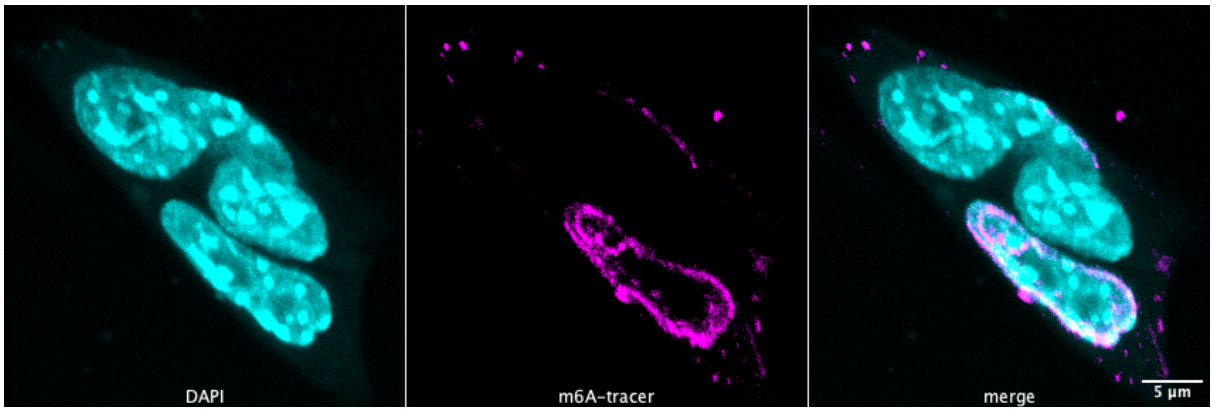

Figure 22. m6A-tracer staining on IB10 Dam-Lmnb1 cells to localize Dam methylation. Scale bar 5µm.

Discussion

Most eukaryotic cells have a conventional nuclear organisation. However the complete opposite is found in rod cells of nocturnal mammals. Here, I describe how mouse retinal organoids can be utilized to study chromatin inversion *in vitro*. By optimizing a published protocol for mROs and developing a transgenic Dam-Lmnb1 expressing cell line, I establish essential prerequisites to study chromatin inversion using DamID.

Pre-culture optimizations

To optimize and investigate the pre-culture conditions, I assessed the treatment of mESC with PD. This showed that addition of PD to mESC during the pre-culture is essential for mRO competence, as only then organoids formed the expected structures, including the characteristic neuroepithelial rim. While I observed a trend towards more mature mRO structures upon prolonged PD treatment, future experiments, focussing on image analysis and quantification of mRO efficiency, will be necessary to draw conclusions.

We observe that higher confluencies presented less differentiating cells during the pre-culture and that organoids showed a thicker neuroepithelial rim as well as a rounder shaper, as well as a higher retinal organoid efficiency compared to the low confluency originating mROs. Nevertheless, future experiments quantifying these observations by immunofluorescence of pluripotency markers in mESCs will be necessary.

While other factors might influence the competence of mESCs, the PD treatment and seeding density were crucial parameters to improve as they directly influenced the organoid culture.

Organoids culture optimizations

The original protocol uses Matrigel, which is time- and resource-prohibitive. Therefore, we focused on Geltrex™ as a suitable alternative for Matrigel™. While I found no morphological differences using Geltrex™, I did not assess differences at the molecular level, which can't be excluded yet before further characterisation.

Published protocols culture mROs at 40% oxygen from day 7 onwards. However, early research by the Kind lab found that mRO's with retinal structures also appeared at 20% oxygen. Our experiment also indicates no major differences between 20% and 40% oxygen levels. However, we only had the opportunity for one experiment under 40% oxygen. Therefore, this comparison would need to be repeated again, to have sufficient replicates for statistical testing.

To compare and verify the competency of the original Dam-LaminB1 F1ES cell line to IB10, we generated mROs with the improved protocol. The F1ES cell line did not yield retinal tissue, as shown by imaging and by qRT-PCR. This highlights a cell line-specific mRO differentiation competence of mESCs and underlines the importance to use IB10 cells.

Chromatin inversion in late organoids

To validate that this inversion in rod cells happens during late stages of organoid culture. DAPI staining on D40 mROs was performed. This type of staining showed the nuclear distribution of the different cell types of the retina layer. More specifically, rod cells already presented the inverted organization while the other cell types with a conventional distribution i.e bipolar cells, kept the same nuclear organization. Therefore, we found that by using our optimized protocol, by D40 IB10 mROs already presented the inversion.

IB10 Dam-LmnB1 cell line generation

To probe lamina-associated domains by DamID-seq, we wanted to include a Dam-LaminB1 fusion protein in IB10. Successful integration was confirmed by qRT-PCR on Dam and rtTA. Moreover, the Methyl-PCR validated that our Tet-On system was functional with a strong signal after eight hours. However, we were unsuccessful in optimizing the degradation by dTAG, which warrants further optimizations. Furthermore, m6A-tracer staining corroborated that this transgenic cell line can be used to study genome-NL interactions since methylated LADs were found at the nuclear periphery. However, further experiments need to validate transgene expression not only in mESCs, but also in mROs.

Finally, by the end of my internship I managed to successfully grow mouse retinal organoids from the new cell line containing the Dam-LmnB1 construct and moreover for the first time identified the inversion phenotype *in vitro*.

To sum up, a functional reporter cell line containing Dam-LmnB1 was generated. This line will be highly valuable for the study of the inversion phenotype during mRO differentiation using DamID analysis. Moreover, future experiments measuring Lmnb1 in comparison to euchromatic histone modifications like H3K4me3 will allow us to investigate the temporal dynamics of euchromatin and heterochromatin changes.

Acknowledgments

First of all, I would like to thank Moritz and Robin for their great supervision during my internship. Their support, enthusiasm and hard work were remarkable. I have learned a lot about the retina, organoids, and cloning. But more importantly, I had the absolute pleasure to learn valuable skills such as scientific writing, optimal time management and presenting.

Next, I would like to thank Jop. Without him this internship would not be possible. It is truly impressive all the single-cell technologies his group has and continues to develop.

Moreover, I would like to thank the whole Kind group. Everyone warmly welcomed me and made me feel part of their team during these past nine months. It was an absolute pleasure and privilege to learn from such good scientists and people.

Last but not least, I would like to thank Jop and Catherine Robin for being my reviewers and taking time and effort to evaluate my internship, report and presentation.

References

Bellapianta, A., Cetkovic, A., Bolz, M., & Salti, A. (2022). Retinal Organoids and Retinal Prostheses: An Overview. *International Journal of Molecular Sciences*, *23*(6). https://doi.org/10.3390/ijms23062922

Briand, N., & Collas, P. (2020). Lamina-associated domains: peripheral matters and internal affairs. *Genome Biology*, *21*(1), 85.

Carter-Dawson, L. D., & LaVail, M. M. (1979). Rods and cones in the mouse retina. II. Autoradiographic analysis of cell generation using tritiated thymidine. *The Journal of Comparative Neurology*, *188*(2), 263–272.

Gargotti, M., Lopez-Gonzalez, U., Byrne, H. J., & Casey, A. (2018). Comparative studies of cellular viability levels on 2D and 3D in vitro culture matrices. *Cytotechnology*, *70*(1), 261–273.

Greil, F., Moorman, C., & van Steensel, B. (2006). DamID: mapping of in vivo protein-genome interactions using tethered DNA adenine methyltransferase. *Methods in Enzymology*, *410*, 342–359.

Hoskins, V. E., Smith, K., & Reddy, K. L. (2021). The shifting shape of genomes: dynamics of heterochromatin interactions at the nuclear lamina. *Current Opinion in Genetics & Development*, *67*, 163–173.

Huisinga, K. L., Brower-Toland, B., & Elgin, S. C. R. (2006). The contradictory definitions of heterochromatin: transcription and silencing. *Chromosoma*, *115*(2), 110–122.

Kim, S., Min, S., Choi, Y. S., Jo, S.-H., Jung, J. H., Han, K., Kim, J., An, S., Ji, Y. W., Kim, Y.-G., & Cho, S.-W. (2022). Tissue extracellular matrix hydrogels as alternatives to Matrigel for culturing gastrointestinal organoids. *Nature Communications*, *13*(1), 1692.

Kind, J., Pagie, L., Ortabozkoyun, H., Boyle, S., de Vries, S. S., Janssen, H., Amendola, M., Nolen, L. D., Bickmore, W. A., & van Steensel, B. (2013). Single-cell dynamics of genome-nuclear lamina interactions. *Cell*, *153*(1), 178–192.

Kind, J., & van Steensel, B. (2010). Genome-nuclear lamina interactions and gene

regulation. *Current Opinion in Cell Biology*, *22*(3), 320–325.

Lochs, S. J. A., Kefalopoulou, S., & Kind, J. (2019). Lamina Associated Domains and Gene Regulation in Development and Cancer. *Cells* , *8*(3). https://doi.org/10.3390/cells8030271

Markodimitraki, C. M., Rang, F. J., Rooijers, K., de Vries, S. S., Chialastri, A., de Luca, K. L., Lochs, S. J. A., Mooijman, D., Dey, S. S., & Kind, J. (2020). Simultaneous quantification of protein-DNA interactions and transcriptomes in single cells with scDam&T-seq. *Nature Protocols*, *15*(6), 1922–1953.

Misteli, T. (2007). Beyond the sequence: cellular organization of genome function. *Cell*, *128*(4), 787–800.

Misteli, T. (2020). The Self-Organizing Genome: Principles of Genome Architecture and Function. *Cell*, *183*(1), 28–45.

Nguyen, K. H., Patel, B. C., & Tadi, P. (2022). Anatomy, Head and Neck: Eye Retina. In *StatPearls*. StatPearls Publishing.

Orian, A., Abed, M., Kenyagin-Karsenti, D., & Boico, O. (2009). DamID: a methylation-based chromatin profiling approach. *Methods in Molecular Biology* , *567*, 155–169.

Osakada, F., Ikeda, H., Mandai, M., Wataya, T., Watanabe, K., Yoshimura, N., Akaike, A., Sasai, Y., & Takahashi, M. (2008). Toward the generation of rod and cone photoreceptors from mouse, monkey and human embryonic stem cells. *Nature Biotechnology*, *26*(2), 215–224.

Ragoczy, T., & Groudine, M. (2009). The nucleus inside out--through a rod darkly [Review of *The nucleus inside out--through a rod darkly*]. *Cell*, *137*(2), 205–207.

Rooijers, K., Markodimitraki, C. M., Rang, F. J., de Vries, S. S., Chialastri, A., de Luca, K. L., Mooijman, D., Dey, S. S., & Kind, J. (2019). Simultaneous quantification of protein-DNA contacts and transcriptomes in single cells. *Nature Biotechnology*, *37*(7), 766–772.

Shevelyov, Y. Y., & Nurminsky, D. I. (2012). The nuclear lamina as a gene-silencing hub. *Current Issues in Molecular Biology*, *14*(1), 27–38.

Shevelyov, Y. Y., & Ulianov, S. V. (2019). The Nuclear Lamina as an Organizer of

Chromosome Architecture. *Cells* , *8*(2). https://doi.org/10.3390/cells8020136

Smith, C. L., Lan, Y., Jain, R., Epstein, J. A., & Poleshko, A. (2021). Global chromatin relabeling accompanies spatial inversion of chromatin in rod photoreceptors. *Science Advances*, *7*(39), eabj3035.

Solovei, I., Kreysing, M., Lanctôt, C., Kösem, S., Peichl, L., Cremer, T., Guck, J., & Joffe, B. (2009). Nuclear architecture of rod photoreceptor cells adapts to vision in mammalian evolution. *Cell*, *137*(2), 356–368.

Solovei, I., Wang, A. S., Thanisch, K., Schmidt, C. S., Krebs, S., Zwerger, M., Cohen, T. V., Devys, D., Foisner, R., Peichl, L., Herrmann, H., Blum, H., Engelkamp, D., Stewart, C. L., Leonhardt, H., & Joffe, B. (2013). LBR and lamin A/C sequentially tether peripheral heterochromatin and inversely regulate differentiation. *Cell*, *152*(3), 584–598.

Tsumura, A., Hayakawa, T., Kumaki, Y., Takebayashi, S.-I., Sakaue, M., Matsuoka, C., Shimotohno, K., Ishikawa, F., Li, E., Ueda, H. R., Nakayama, J.-I., & Okano, M. (2006). Maintenance of self-renewal ability of mouse embryonic stem cells in the absence of DNA methyltransferases Dnmt1, Dnmt3a and Dnmt3b. *Genes to Cells: Devoted to Molecular & Cellular Mechanisms*, *11*(7), 805–814.

van Steensel, B., & Belmont, A. S. (2017). Lamina-Associated Domains: Links with Chromosome Architecture, Heterochromatin, and Gene Repression. *Cell*, *169*(5), 780–791.

Völkner, M., Kurth, T., Schor, J., Ebner, L. J. A., Bardtke, L., Kavak, C., Hackermüller, J., & Karl, M. O. (2021). Mouse Retinal Organoid Growth and Maintenance in Longer-Term Culture. *Frontiers in Cell and Developmental Biology*, *9*, 645704.

Völkner, M., Zschätzsch, M., Rostovskaya, M., Overall, R. W., Busskamp, V., Anastassiadis, K., & Karl, M. O. (2016). Retinal Organoids from Pluripotent Stem Cells Efficiently Recapitulate Retinogenesis. *Stem Cell Reports*, *6*(4), 525–538.

Yu, Y., Wang, X., Zhang, X., Zhai, Y., Lu, X., Ma, H., Zhu, K., Zhao, T., Jiao, J., Zhao, Z.-A., & Li, L. (2018). ERK inhibition promotes neuroectodermal precursor commitment by blocking self-renewal and primitive streak formation of the epiblast. *Stem Cell Research*

& Therapy, *9*(1), 2.

Zheng, H., & Xie, W. (2019). The role of 3D genome organization in development and cell differentiation. *Nature Reviews. Molecular Cell Biology*, *20*(9), 535–550.